Egyptian Journal of Chemistry

http://ejchem.journals.ekb.eg/

Novel Azo Dye Based on 1,3,4-Thiadiazole: Synthesis, Characterization Linked to Application as Dye-Sensitized Solar Cells and Antioxidant

Ashraf M. Ashmawy[1]*, **Amr A. Sayed Alahl**[3], **Ali A. Ali**[1],
Ammar M. Mahmoud[1], **Sameh A. Rizk**[2]

[1] *Chemistry Department, Faculty of Science (boys), Al-Azhar University, Egypt.*

[2] *Chemistry Departments, Faculty of Science, Ain Shams University, Cairo, Egypt.*

[3]*Renewable Energy Department, Desert Research Center, Cairo, Egypt.*

Abstract

In this work, the important features, electrochemical, optical and thermal stability as antioxidant, of four new donor-acceptor–π–acceptor-donor architecture, antioxidant dyes based on thiadiazole were studied. The four dyes carry aryl amino groups as the donors, two 1, 3, 4-thiadiazole moieties as the acceptors and azo and phenyl groups as π spacers. The effect of different aryl amino substituents as the donor group on optimization molecules, geometric, optical properties and electronic properties were studied and discussed. These azo dyes were synthesized by diazotization of 1, 4-bis (2-amino-1,3,4-thiadiazole) benzene and coupling with different aromatic compounds, and their structures were recognized by UV spectroscopy and 1H NMR, FTIR, and elemental analysis. Interestingly, these compounds proved to be as important for lubricants as antioxidants. Outcome of run Density functional theory DFT-based quantum calculations on these dyes so allow comprehensive information in correlation with their cell high performance. Electron donor substrate based on organic solar cells shows power conversion efficiency (PCE) of 5.3 % with 0.93 as high open-circuit voltage by simple solution spin-coating manufacturing procedure. The efficiency of the prepared azo day passes to inhibition base oil from oxidation.

Keywords: Bis-azo-1, 3, 4-thiadiazoles; DFT; antioxidants; lubricant oils; solar cells.

1. Introduction

Due to expanding worldwide energy requests and the turn down in natural energy assets, scientists have focused much attention on improving solar energy production in latest years. Amongst numerous technologies of solar energy, organic photovoltaic cells and dye-sensitized solar cells (DSSCs) are of extraordinary interest due to their excellent efficiencies of energy conversion and low manufacture costs contrasted with those of regular solar cells based on inorganic silicon. Up to now, efficiencies of DSSCs conversion in excess of 11%, have been achieved with dyes of ruthenium complexes [1,2]. Organic metal-free dyes have gotten a lot of consideration as a result of their high molar extinction coefficients, low cost, synthetic flexibility, and achieve requirements of environmental safety. Organic dyes efficiencies have been indicated with variety starting 5% to 10.3% [3,4]. Symmetrical systems in Previous works have revealed with the purpose of a lower concentration of some compounds known as co adsorbent as deoxycholic acid (DCA) and chenodeoxycholic acid (CDCA) already acting a considerable role in enhancement efficiency [5].

Those through the donor-π-acceptor (D-π-A) architecture [6] are shows potential attributable to their absorption for long-range. In addition to the D–π–A colours, organic colorants containing an additional acceptor group, D – A–π–A, have recently been reported [7]. Supplementary acceptor performs as trap for electron and makes possible transfer donor moiety electron to the terminal acceptor/anchor grouping. Dyes of D—A—π—A have benefits such as enhanced photo- and thermal stability, red shifted absorption and

high open-circuit voltage[8]. The simplicity in modification photovoltaic, electrochemical and photophysical properties by altering the acceptor π-bridge and donor, moieties attributed to a variety of entities, such as3-indoline [9,10], ,carbazole [11], phenothiazine[12], and triphenylamine [13,14]which used as donor groups. Moieties such as thiophene [15] ,methane and benzene [16-18]are used as electron-deficient groups, and π-spacers including cyanoacetic acid [19,20]or rhodanine-3-acetic acid [21]. Numerous electron-withdrawing groups, such as quinoxaline [22], benzotriazole [23,24], benzothiadiazole [25-27], diketopyrrolopyrrole [28,29], thienopyridine [30], 1,3-thiazole [31] and dithiazole [32]have been utilized as supplementary acceptor units.

Thiadiazole has been investigated extensively because it has a similar amount of valence electrons as thiazoles, thiophenes, and pyrazines, as well as similar molecular structures. When employed in electrical and photovoltaic applications, the thiadiazole exhibits appealing features [33].

Their optical harvesting, on the other hand, is ineffective when compared to thiazoles. As a result, they've been allied as acceptors in the solar cells production, as well as for their electrical and optical properties. As a result, derivatives of thiadiazoles have been progressively more exploited as an active structure in a variety of applications in polymer chemistry, industrial chemistry, and pharmaceutical chemistry [34–36]. More research has been done on the use of thiadiazole in solar cells. Molecules containing fluorine on both ends of 1,3,4-thiadiazole have been explored in solar applications [37].

It was reported that alternating alkoxy substituents benzothiadiazole and carbazole repeat units with two nearby bithiophene or thiophene units were used to construct new highly processable donor-acceptor polymers [38]. The repeated monomeric units of 1,3,4-thiadiazole structural with grapheme Nano flakes(GNFs) and phenanthrene at both ends was studied [39]. Also two new wide-bandgap co-polymers based on benzoin[1,2-b:4,5-b′] dithiophene and1,3,4-thiadiazole, for constructing particularly efficient non-fullerene organic solar cells (NF-OSCs)was designed and synthesize [40]. Another molecular variation, which can get better orbital strengthen and coupling dye– semiconductor interaction, is the increase of anchoring groups number [41]. This approach was adopted since the first studies on DSCs with cyanines and squaraines groups with symmetrical dianchored dyes [42].

DFT is one of the investigative methodologies most usually utilized for computing compound reactivity of solids and particles [43,44].Many additives of lubricating comprise compounds containing N and their derivatives [45], Such as

benzotriazole derivatives, 1,3,4-thiadiazole derivatives, oxazolone, thiazolino and imidazoline.

Herein, the synthesis of four novel D-A–p–A- D kind dyes (1–4), with various acceptor/anchor groups, were reported. Additionally, were evaluated as antioxidant. Their structural characteristics were studied using DFT which is a semiempirical molecular orbital program was in use to explore their performance as antioxidant additives. The dyes consist of an aryl amine group as the donor, 1, 3, 4-thiadiazole as the acceptor and azo and vinyl groups as π-spacers. An amino group is used as the acceptor/anchor group in dyes.

2. Experimental

2.1. Materials And Instrumentation

High purity chemicals were purchased from worldwide providers. Anhydrous DMF was used thiosemicarbazide, terephthalic acid, potassium hydroxide, 2-naphthyl amine, phosphorus oxychloride and 3- chloroaniline. The analytical reagent grade solvents were used without further purification. Distilled water was used in all experiments. Sodium nitrite, potassium hydroxide and sulfuric acid were obtained from Elnasr Pharmaceutical and Chemical Co. (ADWIC), Egypt. The base oil fraction used in the study was delivered from the Egyptian Petroleum Company and complete characterization in table 1.

Table 1: The physicochemical properties of the Base oil.

Test	Result	Test method
Density @ 15.5°C, g/L	0. 817	ASTM D − 1298
Pour Point, °C	zero	ASTM D − 97
Viscosity at 40°C at 100°C	52.34	ASTM D – 445
	7.41	ASTM D – 445
Viscosity Index (VI)	92	ASTM D – 2270
Total Acid Number (TAN)	0.067	ASTM D – 664
Sulfur Content, wt. %	0.34	ASTM D – 4294
Color	2.5	ASTM D – 1500
Ash Content, wt. %	0.003	ASTM D – 482
Copper Corrosion	I a	ASTM D – 130
Flash point, °C	220	ASTM D – 92
Aniline point °C	100.5	ASTM D – 611

Bruker Vance used to record NMR spectra (400 MHz) spectrometers. Chemical shifts δ are measured in parts per million (ppm) compared with tetramethylsilane, and in Hz are reported coupling constants J. Splitting patterns are defined as small singlet (br s), singlet (s), duplicate (dd), or doublet (d). Absorption spectra were reported on a spectrophotometer visible to the JascoV-

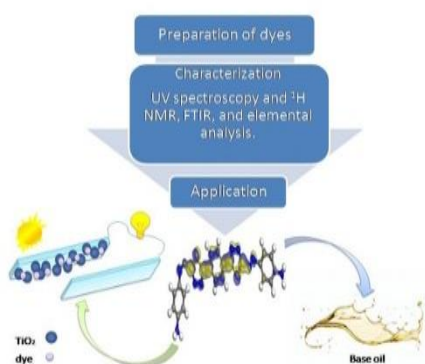550 UV. The experimental part can be conclusion in figure 1.

Figure (1): Step for experimental part.

2.2. Material Preparation:
2.2.1. Synthesis Of 5, 5'-(1, 4-Phenylene) Bis (1, 3, 4-Thiadiazol-2-Amine):

Preparation according to reference [46]. In which a mixture of 0.01 mole of terphthalic acid, 0.02 mole of thiosemicarbazide and 5 mL of phosphorus oxychloride was refluxed gently for 3 hours. The mixture was cooled to room temperature and then 50 ml of ice water was added and the new mixture was also refluxed for 4 hours. Since the phosphoric acid resulting from the chemical reaction makes the dyes soluble, it was necessary to neutralize it with potassium hydroxide; therefore, the mixture was filtered. The solid product was also filtered using filter paper to isolate the insoluble dye from the solution and then it was washed with distilled water. The hot DMF used to rinse residual solid product, then product was left to dry at room temperature.

2.2.2. General Procedure For The Synthesis Of Dyes 1–4

(0.76 g) sodium nitrite was add to cooled 0 °C (5ml) sulfuric acid, in an ice bath to prepare nitrosyl sulfuric acid, and 5,5'-(1,4-phenylene)bis(1,3,4-thiadiazol-2-amine) (0.01 mole)was added portion-wise with stirring. Then, acetic acid–a propionic acid mixture (4:1, 10 ml) was added to the diazonium salt, and the temperature was maintained at 0±5 °C for 2 h. The obtained clear solution of diazOnium was added at 5°C to a (0.02 mole) stirred aryl amine solution in acetic acid–propionic acid mixture (4:1, 20 ml), and the reaction was maintained at pH 4 by sodium acetate portion-wise addition. Later than a tiny moment, the mixture of reaction was decanted into ice water and filtered. The prepared compounds were rinsed on the filter paper with water, and recrystallized after drying [47].

2.3. Computational Studies

B3LYP/6-311G (d, p) density functional theory (DFT) were used to Optimize, The geometries of ground-state **of 1**–**4** dyes. A vibrational analysis was carried out to confirm whether the optimized geometries of the dyes were local energy minima using various functional, such asCAM-B3LYP, M06-2X, LC-WPBE, LC-BLYP, and WB97XD, with a 6-311+G(d,p) basis set in the chloroform solvent using the SCRF(PCM) method [48]. The TZVP basis set andthePBE0 functional was used to optimize the dye geometry of ground-state. The Gauss Sum 2.2 program was used analyze the density of states [49]. Gaussian 09 software utilized to perform all the calculations [50].

2.4. Antioxidant Screening

The oxidation tests were accomplished according to the ASTMD-943standard method. The pure oxygen (99.95%) was used to oxidize 200 ml of base oil, with wires of iron and copper as catalysts. The oxidations were performed at 120 °C at 0.1 l h−1flow rate for a maximum of 96 h. Compounds1–4were added at various concentrations (200, 400, and 500ppm).The evaluation of oil samples were carried out(after 24, 48, 72, and 96 h) through the vary in the total acid number (TAN). The consideration used for the oxidized samples were those in line with test methods D-664 of ASTM standard [51].

3. Results and Discussion
3.1. Design And Synthesis

All the (**1**–**4**) dyes in scheme 1 were synthesized in good yields in two step synthetic path way. In brief, 5,5'-(1,4-phenylene)bis(1,3,4-thiadiazol-2-amine)) underwent diazotization with *in situ*-generated nitrosyl sulfuric acid and subsequent coupling with the appropriate aryl amine to give **1**–**4** in yields of 73–83%.
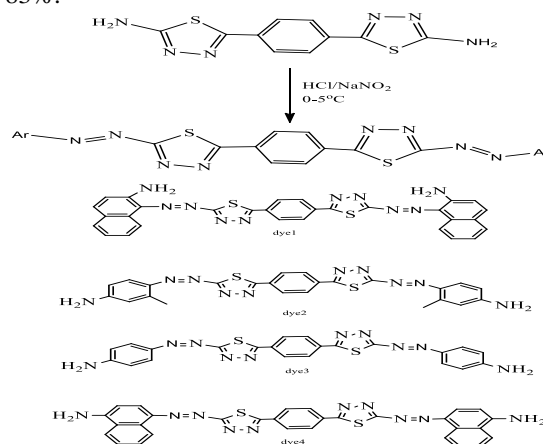
Scheme (1): Synthesis and Chemical structures of bis-azo-1,3,4-thiadiazole dyes **1**–**4**.

3.2. Chemical And Spectral Assignment Of Dye 1, 1,1'-((5,5'-(1,4-phenylene) bis(1,3,4-thiadiazOle-5,2-diyl))bis(diazene-2,1-diyl))bis(naphthalen-2-amine) (dyes 1).

The product appears as yellow crystal with a yield 85% and its structure is confirmed by the following:

- The ^{1}HNMR(400 MHz, DMSO-d_6), δ, ppm,(J, Hz):7.36(2H, dd, J = 8.4 Hz, 5,6 − CH(Ph)), 7.40 (4H, s, 2 (3,4-CH) (naph)), 7.41 (4H, dd, 2(5,6-CHnaph)), 7.43 (2H, dd, J = 7.8 Hz, 2,3 − CH (Ph)), 7.52-7.50 (4H, dd, J = 7.8 Hz, 2(7,8-CH(naph)), 10.45 (4H, bs, 2-NH$_2$) exchangeable D$_2$O. (see in figure 2)
- FTIR(KBr) shows absorption bands (in cm^{-1}) at 3380 and 1510 ν (NH) and δ (NH), 3052 ν (C − H, ar.), 1686 ν(C=N), 1420 ν (C=C ar.), 1014 ν (=N-N=), 732 δ(C-S-C).
- Elemental analysis is C (61.61), H (3.65), N (23.66), and S (10.77).
- Absorption is λ max in DMF/H$_2$O is 552.
- Mass spectra of dye 1 gave molecular ion peak at m/z 584.13 (100%).
- Melting point equal **300**°C.

6,6'-((1E,1'E)-(1,4 − phenylene, bis(1,3,4 − thiadiazole − 5,2 − diyl))bis(diazene-2,1-diyl))bis(3-methylaniline) (Dye 2): The product appears as red crystal with a yield 73% and its structure is confirmed by the following:

- The ^{1}H NMR (400 MHz, DMSO − d$_6$) , δ, ppm, (J, Hz): 2.54(6H, s, 2(CH$_3$Ar), 7.36 (2H, dd, J = 7.4 Hz, 5,6 − CH(Ph)), 7.40 (4H, s, 2 (2,4-CH) (Ar)), 7.41 (2H, d, 2(5-CHnaph)), 7.43(2H, dd, J = 7.4 Hz, 2,3 − CH (Ph)), 9.86 (4H, bs, 2-NH$_2$) exchangeable D$_2$O(see in figure 3).
- FTIR (KBr) shows absorption bands (in cm^{-1}) at 3428 and 1554 ν (NH) and δ (NH), 3055 ν (C − H, ar.), 1616 ν(C=N), 1456 ν (C=C ar.), 1039 ν (=N-N=), 684 δ(C-S-C).
- Elemental analysis is C (56.03), H (3.93), N (27.52), and S (12.51).
- Absorption is λ max in DMF/H$_2$O is **501.**
- Mass spectra of dye 2 gave molecular ion peak at m/z **512.13** (100%).
- Melting point is **200-203** °C.

2,2'-((1E,1'E)-(1,4 − phenylene, bis(1,3,4 − thiadiazole − 5,2 − diyl))bis(diazene-2,1-diyl))di-aniline (Dye 3): The product appears as yellowish crystal with a yield 83% and its structure is confirmed by the following:

- The ^{1}H NMR(400 MHz, DMSO − d$_6$), δ, ppm, (J, Hz): 7.36(2H, dd, J = 8.2 Hz, 5,6 − CH(Ph)), 7.40 (4H, s, 2 (3,4-CH) (ani)), 7.41 (4H, d, 2(5,6-ani)), 7.43(2H, dd, J = 8.2 Hz, 2,3 − CH (Ph)),

9.75 (4H, bs, 2-NH$_2$) exchangeable D$_2$O.(see in figure 4)
- FTIR (K Br) shows absorption bands (in cm^{-1}) at 3379 and 1503 ν (NH) and δ (NH), 3063 ν (C-H, ar.), 1620 ν(C=N), 1414 ν (C=C ar.), 1015 ν (=N-N=), 690 δ(C-S-C).
- Elemental analysis is C (54.53), H (3.33), N (28.91), S (13.23)
- Absorption is λ max in DMF/H$_2$O is **361.**
- Mass spectra of dye **3** gave molecular ion peak at m/z **484.10**(100%) (M^{+1}).
- Melting point equal **284**°C.

2,2'-((1E,1'E)-(1,4-phenylene bis(1,3,4-thiadiazole-5,2-diyl))bis(diazene-2,1-diyl))bis(naphthalen-1-amine) **(Dye 4):**
The product appears as scarlet red crystal with a yield 76% and its structure is confirmed by the following:

- The ^{1}H NMR (400 MHz, DMSO − d$_6$), δ, ppm, (J, Hz): 7.23 (2H, dd, J = 8.1 Hz, 5,6-CH(Ph)), 7.54 (4H, s, 2 (3,4-CH) (naph)), 7.74 (4H, d, 2(5,6-CHnaph)), 7.93 (2H, dd, J = 8.1 Hz, 2,3-CH (Ph)), 7.92-8.00 (4H, dd, J = 8.1 Hz, 2(7,8-CH(naph)), 10.45 (4H, bs, 2-NH$_2$) exchangeable D$_2$O. (see in figure 5)
- FTIR (K Br) shows absorption bands (in cm^{-1}) at 3380 and 1510 ν (NH) and δ (NH), 3052 ν (C-H, ar.), 1686 ν(C=N), 1420 ν (C=C ar.), 1014 ν (=N-N=), 732 δ(C-S-C).
- Elemental analysis is C (61.31), H (3.45), N (23.96), S (10.97)
- Absorption is λ max in DMF/H$_2$O is **494.**
- Mass spectra of dye **4** gave molecular ion peak at m/z **584** (M^{+1})
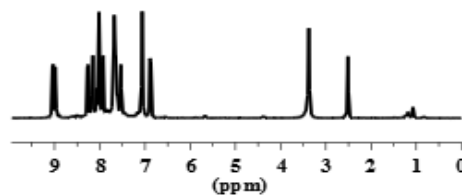- Melting point equal 300°C.

Figure (2). Outline the 1H-NMR of the synthesized highly conjugated Dyes 1.
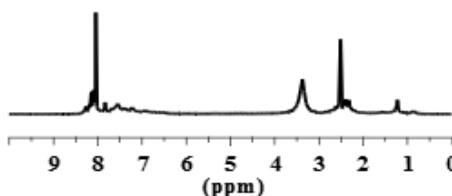

Figure (3): Outline the 1H-NMR of the synthesized highly conjugated Dyes 2.

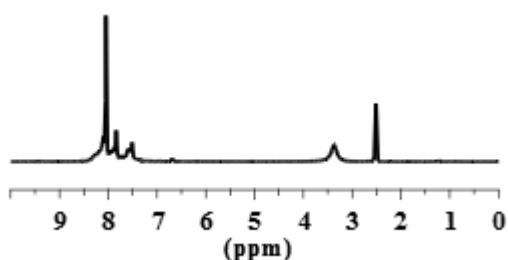**Figure (4):** Outline the 1H-NMR of the synthesized highly conjugated Dyes 3.
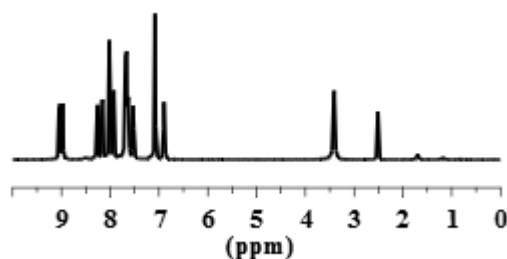

Figure (5): Outline the ^{1}H-NMR of the synthesized highly conjugated Dyes 4.

3.3. Computational Studies

The gas phase at B3LYP/$6-311G(d,p)$ is chosen to perform molecular orbital analysis for all synthesized dyes. The distribution of electron density for the HOMO and LUMO of 1-4 dyes are revealed in Figure 6, all the four dyes HOMO levels are localized on the donor moiety, while the LUMO it is localized on the A–p–A moiety. LUMO of Dyes **1**, **3** and **4** is localized on the 1,3,4-thiadiazole anchoring group. In levels of HOMO and LUMO, the noticed distribution of electron density for dyes on the bridging units proposes effective photo-driven excitation in the transfer of charges. The energy levels HOMO and LUMO, well-separated distribution by electron density suggested that the transition between these stages could be viewed as an excitation in the transfer of energy. Of the CAM-B3LYP and M06-X tests using functionals, they are in strongly agreed with investigational data. The high oscillator strengths of two low energy transitions and dipole moments of ground state are listed in **Table 2**. The transition with low energy corresponds to electron excitation to LUMO from HOMO as the major component that decreases the tendency of charge transfer.

3.3.1. DFT-Based Characterization

The wholly optimized geometrical configurations with minimum-energy of the most potent sensitizing dyes are shown in figure 6 High HOMO energies (E_{HOMO}) are well known to show a molecule strong tendency to electrons donation. Low energy gap values

($\Delta E = E_{LUMO} - E_{HOMO}$) would correspond to great efficiencies for the reason that the needed energy to electron detach, from the last orbital occupied, is small[49]. The linear relation between the energy level of E_{HOMO} and the efficiency indicates that the lower the E_{HOMO} (more negative) of these 1,3,4-thiadiazole derivatives, the higher the ability to accept electrons. Directly proportional to output are the orders of declining E_{HOMO} values and rising E_{LUMO} and ΔE values. The electron cloud tendency to detach itself from its original shape is called its polarizability The more effectively the molecules would be removed from the bulk to form an active film This expanded area improves the ease at which the cloud of electrons distorts, which in turn promotes absorption.; DFT-based quantum calculations will provide insight into organic molecules' structural and electronic characteristics [48].The parameter values resulting from a DFT analysis of 1,3,4-thiadiazole derivatives are the molecular orbitals energy at the frontier. HOMOs represent the electrophilic attacks regions. While nuclear attack regions are the LUMO. E_{HOMO} is a parameter specifically related to the potential for ionization, and its value reflects the sensitivity of organic molecules to electrophile attacks. In comparison, E_{LUMO} is a measure of the affinity of electrons, and its value reflects a nucleophilic attack tendency of molecule's. These parameters achieved through optimize molecule geometrically in first and then those parameters are determined. Figure 6 reveals the distributions LUMO and HOMO. Clearly, the HOMOs are spread over the arylidene and aryl groups, while the LUMOs are found on the 1,3,4-thiadiazole moiety; this is a general phenomenon for the four compounds that are the most active electron transfer centers of the compounds being examined (either electron donation or acceptation). Figure 7(A) illustrates the obtained values of EHOMO and ELUMO for the synthesized molecules. The reported findings indicate that the energy gap ΔE values are in the series of 3 <2 < 4 < 1. This is representative of the reactivity of organic compounds to better surfaces. The low ΔE values, molecules are usually referred to as soft molecules and those with high values are referred to as hard molecules. Actually, reactivity of soft molecules to surface radicals are more compared to hard molecules and give electrons readily to the surface [52].The order of these derivatives was 1 > 4 >2> 3, which was proportionate with the values order of EHOMO to maximize efficiency, Suggesting the scavenging capacity of dyes' depended on the hetero atoms number, in addition to EHOMO values, lipophilicity, surface area and distribution of electrons.

A nucleophilic attack tendency of molecule's. Quantum chemical parameter measurements are in perfect accordance with the performance using the DFT process used for measuring the synthesized compounds. The surface area, softness, hardness, and dipole moment for amino groups carrying 1,3,4-thiadiazole derivatives was compatible with an outstanding efficiency [49]. Conversely, the transferred electrons A and ionization potential I suggest that the highest value of charge density distribution ΔN of 0.114 eV (for 1,3,4-thiadiazole 3) illustrates the maximum electrons transfer, and hence, scavenging radicals superior tendency, means that compound 3 has the highest efficiency. Additionally, the softness σ [eV−1] and hardness ή [eV mol−1].
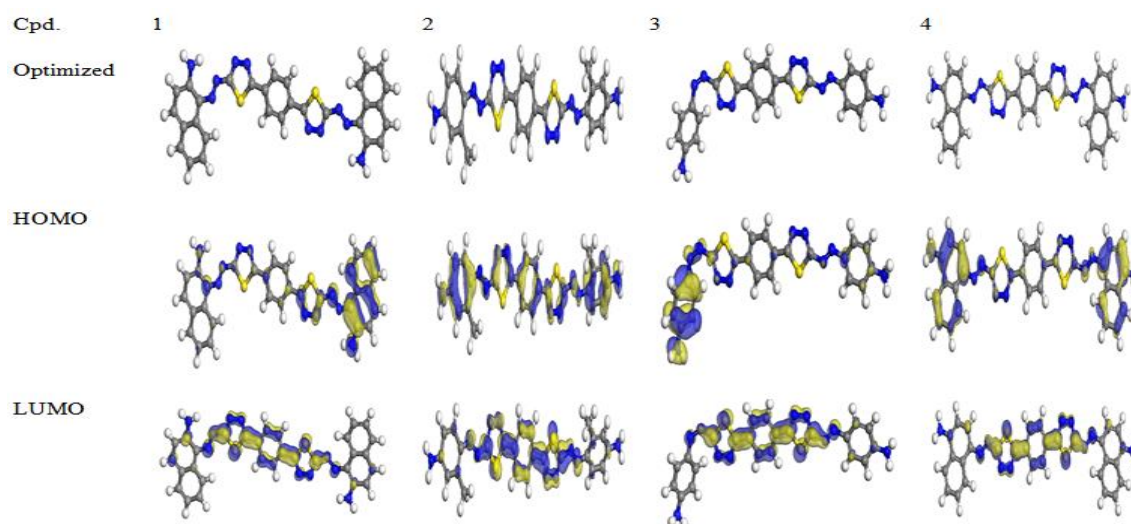

Figure (6): Optimized structures (left), HOMOs (center) and LUMOs (right) obtained for the synthesized compounds;   white=H, gray=C, blue=N, yellow=S.
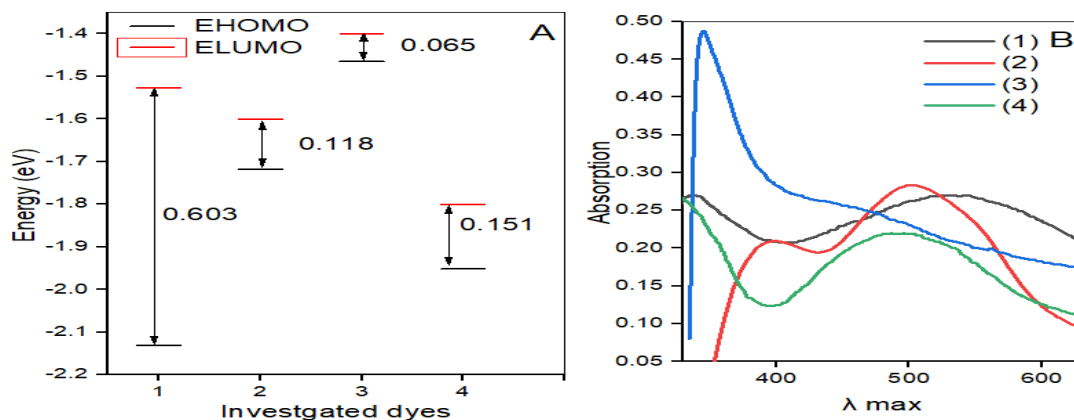

Figure (7): (A) computed energy levels and homo_ lumo gaps   (B) UV/Vis absorption spectra of dyes 1-4 in DMF: H₂O solvent.

Table 2: Quantum chemical parameters calculated for compounds 1–4.

Cpd.	E_{HOMO}	E_{LUMO}	ΔE	I	A	χ	η	σ	ΔN	μ
1	-2.131	-1.528	0.603	2.131	1.528	1.829	0.302	3.301	0.052	1.758
2	-1.718	-1.600	0.118	1.718	1.600	1.659	0.118	8.471	0.068	2.3116
3	-1.466	-1.401	0.065	1.466	1.401	1.4335	0.065	15.381	0.114	2.4278
4	-1.952	-1.801	0.151	1.952	1.801	1.877	0.151	6.625	0.062	1.879

3.4. Absorption Studies of UV Visible Spectroscopic

Dyes 1–4 absorption spectra are revealed in Figure. 7(B). The spectra obtained in DMF: H_2O solvent show bands at approximately (345,569), (404,508), (347,455) and (309,492) nm for dyes 1, 2, 3 and 4 respectively. The bands at (345,404,347 and 309) nm represent π-π* (for π -bond electrons) transitions from two azo group to the thiadiazole moiety and too this region corresponding to the intense benzene, while the bands at (569,508,455 and 492) nm are ascribed to n-π* (for lone pair)transitions from amino group [53]. Change in position of amino group in dyes (1 and 4) produces bathochromic shift in the absorbance of band about 77 nm in the Figure. 7 (B).,because may be near amino group from azo group in dye 1 about dye 4.There is a $\pi - \pi^*$band shift of dyes2 and 3, at 347 nm bathochromic ally to 404 nm, as reason for the electron-donating effect of the methyl group on the benzene moiety[54,55].Ultraviolet(UV) light causes an excitation of an electron from the HOMO to the LUMO in conjugated double bond in disperse dyes. When the electron is excited into the LUMO, the energy level becomes the HOMO- star. Therefore, less energy required for the more highly conjugated level to excite an electron from the HOMO to the LUMO. Conjugation shifts absorption of ultraviolet to longer wavelengths and reduces the HOMO-LUMO gap. The considered molecular Orbitals were the highest (HOMO) occupied and second highest (HOMO-1) ones and the lowest (LUMO) and second lowest (LUMO1) unoccupied ones. Figure. 7 (A). illustrates the (HOMO & LUMO) frontier molecular orbitals of compounds 1-4. In general, the structures are characterized by comparatively low down energies for HOMO and LUMO[56].These results show that during the HOMO relative to LUMO transition of electron more energy is involved. The EHOMO & ELUMO variation produce the energy of band gap (ΔE), which is a significant stability indicator. A band gap with lesser values a measure of a higher probability of electrons transfer within a certain system. dyes 2 and 3 gave the lesser energies of band gap 0.118 and 0.065 eV, respectively [57].

The optimal concentration of the best additive was 500 ppm (Table 3), and the arrange of-azo derivatives efficiency of inhibition was 3 > 2 > 4 > 1, consistent with the order of efficiency as shown in figure 7. Most of the thiadiazole compounds were maximally efficient as antioxidants at the concentration of 400 ppm (Table 3), and The arrange of increased inhibitory activity of 1,3,4-thiadiazoles suggests their capacity to scavenge oxygen, positive holes and Radicals depended not only on the values of E_{HOMO} but also on the hetero atoms number, the availability of electrons,

the surface area and lipophilicity. E_{HOMO} high values are probable to show the strong electrons donation tendency of a molecule. The low energy gap ΔE values should result in good efficiencies of inhibition. The dipole moment, for the 1,3,4-thiadiazole compounds carrying amino groups correlated well with their oxidation inhibition efficiencies. Conversely, the transferred electrons A, charge density distribution ΔN values of 0.57 and 0.34 for compounds 3 and 2, and ionization potential I, indicate the optimal transfer of electrons, respectively. Consequently, its greater ability to scavenge radicals reveals that compound 3 is the most effective antioxidant. In addition, the values of hardness ή and softness suggest that a hard molecule is less reactive than a soft molecule due to a smaller energy distance in a soft molecule. Due to strong relations in both the experimental and calculated antioxidant efficiencies, certain variables disregarded as constant solubility, competitive adsorption, and material behavior may explain why a stronger correlation is not achieved.

Table 3: TAN variation with oxidation time at different additive concentrations.

code	Conc. [ppm]	Total acid number [mg KOH per g sample $\times 10^2$]			
		Oxidation time [h]			
		24	48	72	96
1	200	80.13	87.12	90.98	204.12
	400	77.53	84.23	86.01	204.34
	500	65.89	80.43	85.64	202.15
2	200	25.21	38.92	45.92	120.87
	400	23.91	22.21	42.89	115.01
	500	19.92	20.52	33.62	112.92
3	200	22.97	35.32	38.01	116.12
	400	15.01	19.65	32.92	105.11
	500	10.82	15.82	29.52	100.82
4	200	60.12	55.05	67.78	195.30
	400	56.67	52.87	61.98	180.12
	500	50.43	49.87	56.01	176.92
Base oil	–	94.02	102.54	120.31	205.12

3.5. Photovoltaic Properties

The manufactured color films hole mobility, was estimated using the technique of space charge limited current (SCLC)[58]. Organic electron mobility values of their molecules were similar for the reported donor material. Thus, it can also be anticipated that synthesized dyes will be a shows potential candidate as electron donor materials for solar cells.

The blends of the manufactured colors with distinct weight ratios of 3: 1 , 2: 1, 1.5: 1,1: 1 and1: 1.5 are used to device efficiency optimization and their

voltage curves versus current density are shown in figure 8(a). The blends of the manufactured colors with distinct weight ratios of 1: 1.5, 1: 1, 1.5: 1, 2: 1 and 3: 1 are used to optimize the efficiency of the device and their current density versus voltage curves are shown in figure 8(b). Because the dye molecules displayed deep HOMO (5.13 eV), the solar cells devices show high V_{oc} of 0.93 V which is similar with BDT based high V_{oc} SM − OSCs. Finally, a PCE of 5.3 % for small molecule is obtained with an open-circuit voltage (V_{oc}) of 0.93 V, spun cast at 1500 rpm. Substituents can be used to adjust levels of the band gap, energy morphology, , material packing and solubility. Also the photovoltaic and photo physical properties investigation shows promising results. The Structural modification of **3** on aryl amino substituents as the donor group has improved the efficiency of power conversion (PCE) of 5.3 % with 0.93 as high open-circuit voltage.
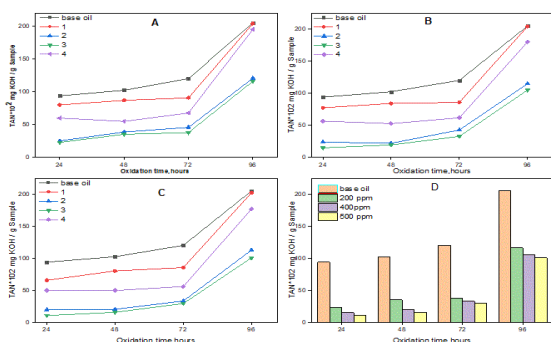

Figure (8): Total Acid Number for base oil with different concentration A) 200 ppm, B) 400 ppm, C)500 ppm and D) Compound 3 with different concentration.
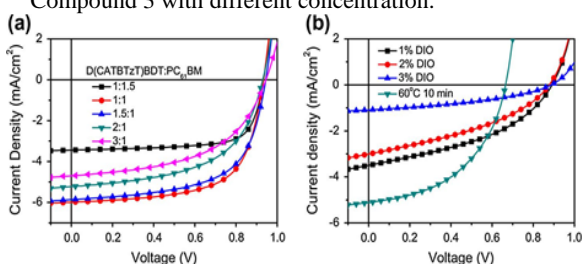

Figure (9): The OSCs Curves based on synthetized dyes under 100 mW/cm², AM 1.5G illumination (a) normal device and (b) DIO treated or thermal annealing devices.

3.5.1. Scaled Up Device- Comparison With Low Concentrator Photovoltaic (**LCPV**) Coupled Device

Usage Dye-sensitized solar cells (DSSCs) as element of building integrated photovoltaic (BIPV), The cells must be made as translucent as feasible, particularly for window apps. Because of this, DSSC scaling has developed in to an significant method even though it has been allied with various problems. Here, DSSC device, active area of 1.1 cm² with transparency

37% and 10 µm thiadiazole thickness was fabricated to study the scale-up device performance. Figure8 (a, b) shows the power density–voltage and current density -voltage behavior respectively for device with an active area of 0.28 cm² and 1.1 cm² (large area than 0.28 cm² with~ 4 times). The device of 1.1 cm² active area gives short circuit current higher than device with small area. However, the present scaled-up DSSC density and energy density is much smaller than the smaller adevices. Because of the high resistance of sheet, which causes loss of ohmic and additionally leads to a considerably reduce in fill-factor as well as efficiency of the scaled-up devices[59].The focused light causes an enhance in the short circuit current. Like silicone solar cells, the DSSC open circuit voltage rises with intensity of light logarithmically relative to the below equation,

$$V'_{oc} = V_{oc} + \frac{nKT}{q} \ln X$$

where X is the sunlight concentration [60].Even though the fill factor reduced relative to the bare cells for all machines, which could be caused by recombination of more electron, but overall efficiency of photovoltaic improved with low concentration for all appliances.

3.6. Spacers Containing Thiadiazole Fragments

Dye with a dual p-conjugated spacer of phenyl dithiadiazolyl precursors have function of the binary spacer is to keep the blocks of both lipophilic heterocyclic-substituted diphenyl amine and hydrophilic amino groups[3]. The DSSC with this amphiphilic dye 3 and 2 exhibited of 10.10%, this has reached an encouraging milestone in organic color growth. The authors can be synthesized four dyes by incorporating the Aryl heterocyclic of phenyl dithiadiazolyl spacer, the pertinent cell exhibits an excellent efficiency of 9.40% with a Fe (II/III) tris(bithiadiazoyl) base delectrolyte as example [58].

4. Conclusions

Four new Thiadiazole dyes with D-A-p-A-D -system were synthesized with various acceptor/anchor and characterized, and their photophysical properties were investigated. Visible region absorption in all the dyes showed excellent light-harvesting capability. The importance of the localization of the LUMO electron density on the acid/anchor group for better interfacial electron injection from the excited-state dyes showed excellent light-harvesting capability. The localization importance of the LUMO electron density on the acid/anchor group for better interfacial electron injection from the excited-state dye to a semiconductor was also investigated by DFT calculations, and all the dyes revealed efficient interfacial electron transfer.

Furthermore, all the dyes exhibited reasonable to good efficiencies in AM 1.5 irradiation. Structural modification of **3** is in progress for enhancement of its photovoltaic and photophysical properties. Overall, our results compare to previous work, display a promising forward toward the efficient D-A-p-A-D molecular configuration, low-price, and facile-fabrication with stable and high-performance.all azo dye pass as antioxidant and dye 3 inhibition efficiency around 90% compared to base oil.

5. References

[1] Y. Numata, S.P. Singh, A. Islam, M. Iwamura, A. Imai, K. Nozaki, L. Han, Enhanced light-harvesting capability of a panchromatic Ru(II) sensitizer based on π-extended terpyridine with a 4-methylstylryl group for dye-sensitized solar cells, Adv. Funct. Mater. (2013). https://doi.org/10.1002/adfm.201202504.

[2] A. Mahmood, Triphenylamine based dyes for dye sensitized solar cells : A review, Sol. energy . 123 (2016) 127–144. https://doi.org/10.1016/j.solener.2015.11.015.

[3] W. Zeng, Y. Cao, Y. Bai, Y. Wang, Y. Shi, M. Zhang, F. Wang, C. Pan, P. Wang, Efficient dye-sensitized solar cells with an organic photosensitizer featuring orderly conjugated ethylenedioxythiophene and dithienosilole blocks, Chem. Mater. 22 (2010) 1915–1925. https://doi.org/10.1021/cm9036988.

[4] Y.S. Yen, H.H. Chou, Y.C. Chen, C.Y. Hsu, J.T. Lin, Recent developments in molecule-based organic materials for dye-sensitized solar cells, J. Mater. Chem. (2012). https://doi.org/10.1039/c2jm30362k.

[5] C. Duarte, M.C. De Oliveira, J.M. Toldo, P. Fernando, B. Gonçalves, M. José, L. Santos, F.S. Rodembusch, Guest-Host Interactions in Symmetrical Carboxy Heptamethine Cyanine Dyes-Titanium Dioxide Systems : Synthesis , Theoretical Calculations , Aggregation Properties , and Application in Dye-Sensitized Solar Cells, 2021 (2021).

[6] A. Mishra, M.K.R. Fischer, P. Büuerle, Metal-Free organic dyes for dye-Sensitized solar cells: From structure: Property relationships to design rules, Angew. Chemie - Int. Ed. (2009). https://doi.org/10.1002/anie.200804709.

[7] Y. Wu, W. Zhu, Organic sensitizers from D-π-A to D-A-π-A: Effect of the internal electron-withdrawing units on molecular absorption, energy levels and photovoltaic performances, Chem. Soc. Rev. 42 (2013) 2039–2058. https://doi.org/10.1039/c2cs35346f.

[8] W. Zhu, Y. Wu, S. Wang, W. Li, X. Li, J. Chen, Z.S. Wang, H. Tian, Organic D-A-π-A solar cell sensitizers with improved stability and spectral response, Adv. Funct. Mater. (2011). https://doi.org/10.1002/adfm.201001801.

[9] D. Kuang, S. Uchida, R. Humphry-Baker, S.M. Zakeeruddin, M. Grätzel, Organic dye-sensitized ionic liquid based solar cells: Remarkable enhancement in performance through molecular design of indoline sensitizers, Angew. Chemie - Int. Ed. 47 (2008) 1923–1927. https://doi.org/10.1002/anie.200705225.

[10] Y. Wu, M. Marszalek, S.M. Zakeeruddin, Q. Zhang, H. Tian, M. Grätzel, W. Zhu, High-conversion-efficiency organic dye-sensitized solar cells: Molecular engineering on D-A-π-A featured organic indoline dyes, Energy Environ. Sci. 5 (2012) 8261–8272. https://doi.org/10.1039/c2ee22108j.

[11] N. Koumura, Z.S. Wang, S. Mori, M. Miyashita, E. Suzuki, K. Hara, Alkyl-functionalized organic dyes for efficient molecular photovoltaics, J. Am. Chem. Soc. (2006). https://doi.org/10.1021/ja0645640.

[12] H. Tian, X. Yang, R. Chen, Y. Pan, L. Li, A. Hagfeldt, L. Sun, Phenothiazine derivatives for efficient organic dye-sensitized solar cells, Chem. Commun. (2007) 3741–3743. https://doi.org/10.1039/b707485a.

[13] Y. Liang, B. Peng, J. Liang, Z. Tao, J. Chen, Triphenylamine-based dyes bearing functionalized 3,4- propylenedioxythiophene linkers with enhanced performance for dye-sensitized solar cells, Org. Lett. 12 (2010) 1204–1207. https://doi.org/10.1021/ol902973r.

[14] D.P. Hagberg, J.H. Yum, H.J. Lee, F. De Angelis, T. Marinado, K.M. Karlsson, R. Humphry-Baker, L. Sun, A. Hagfeldt, M. Grätzel, M.K. Nazeeruddin, Molecular engineering of organic sensitizers for dye-sensitized solar cell applications, J. Am. Chem. Soc. 130 (2008) 6259–6266. https://doi.org/10.1021/ja800066y.

[15] H. Choi, C. Baik, S.O. Kang, J. Ko, M.S. Kang, M.K. Nazeeruddin, M. Grätzel, Highly efficient and thermally stable organic sensitizers for solvent-free dye-sensitized solar cells, Angew. Chemie - Int. Ed. (2008). https://doi.org/10.1002/anie.200703852.

[16] K. Hara, T. Sato, R. Katoh, A. Furube, T. Yoshihara, M. Murai, M. Kurashige, S. Ito, A. Shinpo, S. Suga, H. Arakawa, Novel conjugated organic dyes for efficient dye-sensitized solar cells, Adv. Funct. Mater. (2005).

https://doi.org/10.1002/adfm.200400272.

[17]   D.P. Hagberg, T. Edvinsson, T. Marinado, G. Boschloo, A. Hagfeldt, L. Sun, A novel organic chromophore for dye-sensitized nanostructured solar cells, Chem. Commun. (2006) 2245–2247. https://doi.org/10.1039/b603002e.

[18]   S. Hwang, J.H. Lee, C. Park, H. Lee, C. Kim, C. Park, M.H. Lee, W. Lee, J. Park, K. Kim, N.G. Park, C. Kim, A highly efficient organic sensitizer for dye-sensitized solar cells, Chem. Commun. (2007) 4887–4889. https://doi.org/10.1039/b709859f.

[19]   K.R.J. Thomas, Y.C. Hsu, J.T. Lin, K.M. Lee, K.C. Ho, C.H. Lai, Y.M. Cheng, P.T. Chou, 2,3-Disubstituted Thiophene-Based Organic Dyes for Solar Cells, Chem. Mater. 20 (2008) 1830–1840. https://doi.org/10.1021/cm702631r.

[20]   Q. Feng, X. Lu, G. Zhou, Z.S. Wang, Synthesis and photovoltaic properties of organic sensitizers incorporating a thieno[3,4-c]pyrrole-4,6-dione moiety, Phys. Chem. Chem. Phys. 14 (2012) 7993–7999. https://doi.org/10.1039/c2cp40872d.

[21]   H. Tian, X. Yang, R. Chen, R. Zhang, A. Hagfeldt, L. Sun, Effect of different dye baths and dye-structures on the performance of dye-sensitized solar cells based on triphenylamine dyes, J. Phys. Chem. C. 112 (2008) 11023–11033. https://doi.org/10.1021/jp800953s.

[22]   K. Pei, Y. Wu, W. Wu, Q. Zhang, B. Chen, H. Tian, W. Zhu, Constructing organic D-A-π-a-featured sensitizers with a quinoxaline unit for high-efficiency solar cells: The effect of an auxiliary acceptor on the absorption and the energy level alignment, Chem. - A Eur. J. 18 (2012) 8190–8200. https://doi.org/10.1002/chem.201103542.

[23]   Y. Cui, Y. Wu, X. Lu, X. Zhang, G. Zhou, F.B. Miapeh, W. Zhu, Z.S. Wang, Incorporating benzotriazole moiety to construct D-A-π-A organic sensitizers for solar cells: Significant enhancement of open-circuit photovoltage with long alkyl group, Chem. Mater. 23 (2011) 4394–4401. https://doi.org/10.1021/cm202226j.

[24]   J. Mao, F. Guo, W. Ying, W. Wu, J. Li, J. Hua, Benzotriazole-bridged sensitizers containing a furan moiety for dye-sensitized solar cells with high open-circuit voltage performance, Chem. - An Asian J. 7 (2012) 982–991. https://doi.org/10.1002/asia.201100967.

[25]   S. Haid, M. Marszalek, A. Mishra, M. Wielopolski, J. Teuscher, J.E. Moser, R. Humphry-Baker, S.M. Zakeeruddin, M.

Grätzel, P. Bäuerle, Significant improvement of dye-sensitized solar cell performance by small structural modification in π-conjugated donor-acceptor dyes, Adv. Funct. Mater. 22 (2012) 1291–1302. https://doi.org/10.1002/adfm.201102519.

[26]   J.J. Kim, H. Choi, J.W. Lee, M.S. Kang, K. Song, S.O. Kang, J. Ko, A polymer gel electrolyte to achieve ≥6% power conversion efficiency with a novel organic dye incorporating a low-band-gap chromophore, J. Mater. Chem. 18 (2008) 5223–5229. https://doi.org/10.1039/b809376h.

[27]   Y. Wu, X. Zhang, W. Li, Z.S. Wang, H. Tian, W. Zhu, Hexylthiophene-featured D-A-π-a structural indoline chromophores for coadsorbent-free and panchromatic dye-sensitized solar cells, Adv. Energy Mater. 2 (2012) 149–156. https://doi.org/10.1002/aenm.201100341.

[28]   S. Qu, W. Wu, J. Hua, C. Kong, Y. Long, H. Tian, New diketopyrrolopyrrole (DPP) dyes for efficient dye-sensitized solar cells, J. Phys. Chem. C. 114 (2010) 1343–1349. https://doi.org/10.1021/jp909786k.

[29]   S. Qu, C. Qin, A. Islam, Y. Wu, W. Zhu, J. Hua, H. Tian, L. Han, A novel D-A-π-A organic sensitizer containing a diketopyrrolopyrrole unit with a branched alkyl chain for highly efficient and stable dye-sensitized solar cells, Chem. Commun. 48 (2012) 6972–6974. https://doi.org/10.1039/c2cc31998e.

[30]   X. Lu, G. Zhou, H. Wang, Q. Feng, Z.S. Wang, Near infrared thieno[3,4-b]pyrazine sensitizers for efficient quasi-solid-state dye-sensitized solar cells, Phys. Chem. Chem. Phys. 14 (2012) 4802–4809. https://doi.org/10.1039/c2cp40441a.

[31]   C.H. Chen, Y.C. Hsu, H.H. Chou, K.R. Justin Thomas, J.T. Lin, C.P. Hsu, Dipolar compounds containing fluorene and a heteroaromatic ring as the conjugating bridge for high-performance dye-sensitized solar cells, Chem. - A Eur. J. 16 (2010) 3184–3193. https://doi.org/10.1002/chem.200903151.

[32]   J. He, W. Wu, J. Hua, Y. Jiang, S. Qu, J. Li, Y. Long, H. Tian, Bithiazole-bridged dyes for dye-sensitized solar cells with high open circuit voltage performance, J. Mater. Chem. 21 (2011) 6054–6062. https://doi.org/10.1039/c0jm03811c.

[33]   A.M. Khudhair, F.N. Ajeel, M.H. Mohammed, Engineering and design of simple models from dye-sensitive of solar cells and photovoltaic cells applications:

Theoretical study, Chem. Phys. Lett. 713 (2018) 166–171. https://doi.org/10.1016/j.cplett.2018.10.014.

[34]   A.E. M.Dadsetani, H.Nejatipour, Abinitio study of the optical properties of crystalline phenanthrene, including the excitonic effects, J. Phys. Chem. Solids. 80 (2015) 67–77.

[35]   R.K.A. A.K.Jain, S.Sharma, A.Vaidya, V.Ravichandran, 1,3,4-thiadiazole and its derivatives: a review on recent progress in biological activities, Chem. Biol. Drug Des. 81 (2013) 557–576.

[36]   H.-L.Z. Y. Hu, C.-Y. Li, X.-M. Wang, Y.-H. Yang, 1, 3, 4-Thiadiazole: synthesis, reactions, and applications in medicinal, agricultural, and materials chemistry, Chem. Rev. 114 (2014) 5572–5610.

[37]   N.F.-H. N.A. Sánchez-Bojorge, L.M. Rodríguez-Valdez, DFT calculation oftheelectronicpropertiesoffluorene-1,3,4-thiadiazoleoligomers, J.Mol.Model. 19 (2013) 3537–3542.

[38]   D.G.L. H. Yi, S. Al-Faifi, A. Iraqi, D.C. Watters, J. Kingsley, Carbazole and thienyl benzo [1, 2, 5] thiadiazole based polymers with improved open circuit voltagesandprocessabilityforapplicationinsolarcells, J.Mater.Chem. 21 (2011) 13649–13656.

[39]   A.Alrikabi, Theoreticalstudyofthedesigndyesensitivityforusageinthesolarcell device, Results Phys. 7 (2017) 4359–4363.

[40]   Q.P. X. Xu, T. Yu, Z. Bi, W. Ma, Y. Li, Realizing over 13% efficiency in green-solvent-processed nonfullerene organic solar cells enabled by 1, 3, 4-thiadiazole-based wide-bandgap copolymers, Adv. Mater. 30 (2018) 1703973.

[41]   C. Saccone, Davide; Galliano, Simone; Barbero, Nadia; Quagliotto, Pierluigi; Viscardi, Guido; Barolo, Polymethine dyes in hybrid photovoltaics: structure- properties relationships, European J. Org. Chem. 13 (2016) 2244–2259. https://doi.org/10.1002/ejoc.201501598.

[42]   J. Park, N. Barbero, J. Yoon, E.D. Orto, S. Galliano, R. Borrelli, J. Yum, D. Di Censo, M. Gr, K. Nazeeruddin, C. Barolo, G. Viscardi, Panchromatic symmetrical squaraines : a step forward in the molecular engineering of low cost, (2014) 24173–24177. https://doi.org/10.1039/c4cp04345f.

[43]   D. Belega, D. Dallet, Multifrequency signal analysis by Interpolated DFT method with maximum sidelobe decay windows, Meas. J. Int. Meas. Confed. (2009). https://doi.org/10.1016/j.measurement.2008.0

8.006.

[44]   Ş. Erdoğan, Z.S. Safi, S. Kaya, D.Ö. Işın, L. Guo, C. Kaya, A computational study on corrosion inhibition performances of novel quinoline derivatives against the corrosion of iron, J. Mol. Struct. 1134 (2017) 751–761. https://doi.org/10.1016/j.molstruc.2017.01.037.

[45]   R.M. Fikry, R.A. El-adly, Some azine and azole derivatives as antioxidant additives for lithium lubricating grease, Egypt. J. Pet. 22 (2013) 61–71. https://doi.org/10.1016/j.ejpe.2012.07.003.

[46]   W.A.A. Arafa, A.F. Abdel-Magied, Utilization of ultrasonic irradiation as green and effective one-pot protocol to prepare a novel series of bis-2-amino-1, 3, 4-oxa(thia)diazoles and bis-tetrazoles, Arkivoc. (2017). https://doi.org/10.24820/ark.5550190.p010.197.

[47]   M.C.R. Castro, P. Schellenberg, M. Belsley, A.M.C. Fonseca, S.S.M. Fernandes, M.M.M. Raposo, Dyes and Pigments Design , synthesis and evaluation of redox , second order nonlinear optical properties and theoretical DFT studies of novel bithiophene azo dyes functionalized with thiadiazole acceptor groups, 95 (2012) 392–399. https://doi.org/10.1016/j.dyepig.2012.05.014.

[48]   Ashmawy, Ashraf M., Ahmed M. El-Sawy, Ali A. Ali, Salah M. El-Bahy, and Amr A. Sayed Alahl. Oxidative stability performance of new azophenol derivatives as antioxidants in working fluids for high-temperature solar applications. Solar Energy Materials and Solar Cells 230 (2021): 111282.

[49]   A.T. El-gendy, A.A. Youssef, S.A. Rizk, Which energetically favorable sustainable synthesis of 4-amino-8-azacoumarin ester or 4-hydroxy-3-cyano derivative based on new exact kinetic Arrhenius and DFT stimulation, J. Iran. Chem. Soc. 17 (2020) 1001–1011. https://doi.org/10.1007/s13738-019-01838-5.

[50]   M. Frisch, G. Trucks, H. Schlegel, G. Scuseria, M. Robb, J. Cheeseman, G. Scalmani, V. Barone, B. Mennucci, G. Petersson, Gaussian 09 software, Gaussian, Inc. Wallingford, CT. (2009).

[51]   A.M. Ashmawy, S.K. Attia, M.I. Nessim, E. sayed M. Elnaggar, A.A. El-Bassoussi, Study on some azo liquid crystals as antioxidants for local base oil, Mol. Cryst. Liq. Cryst. 668 (2018) 78–90.

[52]   Kamal, A. B., Mostfa, M. A., Ashmawy, A. M., El-Gaby, M. S. A., & Ali, G. A. (2022).

_____

Corrosion inhibition behavior of the synthesized pyrazoline-sulfonamide hybrid of mild steel in aqueous solutions: experimental and quantum investigations. *Journal of Chemical Sciences, 134*(3), 1-14.

[53]   Kowalski, K., et al., Synthesis, structure, and spectroelectrochemistry of ferrocenyl–meldrum's acid donor–acceptor systems. Organometallics, 2014. 33(18): p. 4697-4705., (n.d.).

[54]   Zhang, Q., et al., Synthesis, crystal structure, electrochemistry and in situ FTIR spectroelectrochemistry of a bisferrocene pyrazole derivative. Dalton Transactions, 2011. 40(14): p. 3510-3516, (n.d.).

[55]   López-Mayorga, B., et al., Ferrocene amphiphilic D–π–A dyes: synthesis, redox behavior and determination of band gaps. New Journal of Chemistry, 2018. 42(8): p. 6101-6113., (n.d.).

[56]   Labulo, A.H., B. Omondi, and V.O. Nyamori, Synthesis, crystal structures and electrochemical properties of ferrocenyl imidazole derivatives. Heliyon, 2019. 5(10):

p. e02580., (n.d.).

[57]   Deglmann, P., A. Schäfer, and C. Lennartz, Application of quantum calculations in the chemical industry—An overview. International Journal of Quantum Chemistry, 2015. 115(3): p. 107-136., (n.d.).

[58]   Y. Hao, X. Yang, J. Cong, H. Tian, A. Hagfeldt, L. Sun, Efficient near infrared D–π–A sensitizers with lateral anchoring group for dye-sensitized solar cells, Chem. Commun. (2009) 4031–4033.

[59]   Y. Hao, X. Yang, J. Cong, H. Tian, A. Hagfeldt, L. Sun, Efficient near infrared D–π-A sensitizers with lateral anchoring group for dye-sensitized solar cells, Chem. Commun. (2009) 4031–4033. https://doi.org/10.1039/b908396k.

[60]   A. Zaban, M. Greenshtein, J. Bisquert, Determination of the electron lifetime in nanocrystalline dye solar cells by open-circuit voltage decay measurements, ChemPhysChem. 4 (2003) 859–864. https://doi.org/10.1002/cphc.200200615.

_____